Comprehensive influences measurement and analysis of power converter low frequency current ripple on PEM fuel cell

Yuedong Zhan[a,*], Youguang Guo[b], Jianguo Zhu[c], Bo Liang[d], Biao Yang[a]

[a] Department of Automation, Kunming University of Science and Technology,

Kunming, 650500, China

[b] School of Electrical and Data Engineering, University of Technology Sydney,

Sydney, NSW 2007, Australia

[c] School of Electrical & Information Engineering, The University of Sydney,

Sydney, NSW 2006, Australia

[d] School of Materials and Energy, Guangdong University of Technology,

Guangzhou, 510006, China

(Emails: ydzhan@163.com, youguang.guo-1@uts.edu.au, jianguo.zhu@sydney.edu.au,

liangbo@gdut.edu.cn, yb_chenggong@163.com)

*Corresponding author: Tel.: +86 871 65916596; Fax: +86 871 65916596, Email

address: ydzhan@163.com (Yuedong Zhan)

ABSTRACT

To deeply understand the influences of power converter's low frequency current ripple (LFCR) and harmonics on a proton exchange membrane fuel cell (PEMFC) in its power conditioning system (PCS), the comprehensive measurement and analysis for the influences of LFCR and harmonics on fuel cell (FC) performances and durability is

investigated in this paper. Based on an equivalent circuit model of PEMFC stack and a

mechanism model for evaluating the LFCR effects on the PEMFC, this paper studies

primarily and systematically the comprehensive influences of LFCR and harmonics on

PEMFC performances and durability, such as (1) degrading the PEMFC performance,

(2) shortening the lifetime of PEMFC, (3) reducing the stack output power, (4) lowing

its availability efficiency, (5) producing more heat and raising the PEMFC temperature,

(6) consuming more fuel, and (7) decreasing the fuel utilization. Finally, a Horizon 300

W PEMFC stack is implemented and tested.

Keywords: Proton exchange membrane fuel cell; Low frequency current ripple; Fuel

cell performance and durability; Power conditioning system

1. Introduction

The proton exchange membrane fuel cell (PEMFC) using hydrogen fuel has a long

continuous run-time, high power density, and low operating temperature, and hence it is

very suitable to be used as a reliable power source in fuel cell (FC) power generation

system (PGS). Since the PEMFC is an electrochemical device, it must employ a power

conditioning system (PCS), e.g. a DC/DC converter to promote the low DC voltage

produced by an FC to a higher one, and/or a DC/AC inverter to obtain an AC voltage.

For instance, a DC/DC converter in an uninterrupted power supply (UPS) system can

boost a low PEMFC voltage of 36 V to ±380 V for the DC/AC inverter, as depicted in
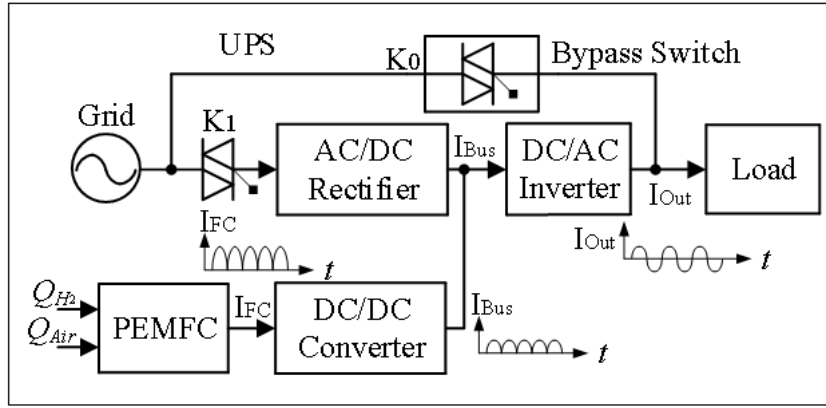
Fig. 1.

Fig. 1.   Schematic diagram of a PEMFC UPS and low frequency current ripples (LFCRs).

As a low voltage and high current device, the low frequency current ripple (LFCR) is a major design issue for a power converter in a PEMFC PGS [1, 2]. The input LFCR must be limited to within 5% of the normal rated value to ensure the satisfactory PEMFC operation. For this reason, the USA National Energy Technology Laboratory published the limits of the LFCR for PEMFC, which suggests that the 100 Hz or 120 Hz ripple should be lower than 15% from 10% to 100% load, not to exceed 0.6 A for lighter loads, and the 50 Hz or 60 Hz ripple should be lower than 10% from 10% to 100% loads, not to exceed 0.4 A for lighter loads [3, 4].

Based on our research findings, the performance and durability influences of LFCR on FC, could be primarily and systematically summarized as that the LFCR is reflected into PEMFC stack and brings harmful influences on the FC stack, such as (1) degrading the FC performance, (2) shortening the lifetime of FC, (3) reducing the stack output power, (4) lowing its availability and efficiency, (5) producing more heat and raising the FC temperature, (6) consuming more fuel, and (7) decreasing the fuel utilization.

The influence mechanisms of the LFCR and harmonics on the FC and the involved electrochemical processes are not completely understood yet, which have become an important subject of investigation. Some research papers can be found in the literature indicating that the LFCR can make the voltage-current performance of FC be a hysteretic behavior and reduce the output power [5-8], it might also decrease the FC durability [3, 9-10], and it can generate harmful influences on FC stack, such as increasing more than 10% of fuel consumption, slowing cathode surface responses, creating oxygen starvation, reducing the operating lifetime, and tripping the overload situation [11-13].

Therefore, to control the high current ripple, limit the LFCR within the desired range, i.e. 5%, and prolong the lifetime of FCs, three main types of ripple current mitigation strategies have been studied in the power conditioning systems (PCS) as the following: (1) Passive compensation approaches, (2) Active compensation approaches, and (3) Passive and active hybrid compensation methods [14].

Regarding the other research work in this field, Ref. [15] proposed an interleaved high gain boost converter topology with a diode clamped multilevel inverter as power interface, which has the main advantages of input LFCR mitigation, high voltage conversion ratio, and voltage balancing across output capacitors. In Ref. [16], based on silicon carbide (SiC) semiconductors and inversely coupled inductors, the proposed 6-phase interleaved boost converter (IBC) has achieved low input LFCR, high efficiency, high compactness, high voltage gain ratio and high redundancy. In Ref. [17],

a fractional order proportional integral (FOPI) controller was designed for regulating the load voltage to achieve the system specification as compared to the classical integer order proportional integral (IOPI) controller, which can improve the PEMFC dynamic performance and reduce the LFCR under different operating conditions. Ref. [18] found that the power converter has a very important role in lowering the performance and efficiency of PEMFC PCS because of the input LFCR. Ref. [19] proposed a control system, which can contribute significantly to increasing the lifetime, efficiency and reliability of FC PGS, despite its input LFCR. Ref. [20] conducted a comparative study for the hydrogen and oxygen concentration for the 60 Hz case of LFCR, when the current amplitude factor increases, so does the deviation from the steady state of the reactant concentration. The oxygen diffusion response is affected, when the hydrogen utilization becomes a severe high current amplitude factor.

The rest of this paper is organized in the following. Section 2 presents the study on the equivalent circuit model, and electrochemical generation steps of electricity in a PEMFC. Section 3 describes the derivation of LFCR production mechanism and model on FC stack. In Section 4, the experimental measurement results obtained from a Horizon 300 W prototype are presented to confirm the influences of LFCR on the PEMFC performance, lifetime, power and efficiency, heat and temperature, fuel consumption and utilization.

2. Equivalent circuit model of PEMFC stack

The PEMFC is a type of electrochemical energy conversion device. If the parameters for each single cell are lumped to represent the PEMFC stack, the output voltage of the stack can be expressed as [21]:

$$V_{stack} = E_{rev} - N\left\{\frac{RT}{\alpha nF}\ln\left(\frac{i+i_n}{i_0}\right) + R_{Ohm}(i+i_n) + \frac{RT}{nF}\left(1+\frac{1}{\alpha}\right)\ln\left[\frac{i_L}{i_L-(i+i_n)}\right]\right\} \qquad (1)$$

where E_{rev} is the reversible voltage (V), N the number of cells in a PEMFC stack, α the transfer coefficient, n the number of electrons per molecule of H_2 (2 electrons per molecule), F the Faraday's constant (C/mol), T the stack or operation temperature (K), R the universal gas constant (J/mol·K), R_{Ohm} the area-normalized resistance, also known as area specific resistance (ARS) of the PEMFC measured (Ω·cm^2), i_0 the exchange current density (A/cm^2), i_n the internal current or parasitic current density that is wasted (A/cm^2), i_L the limiting current density at which the cell voltage will fall rapidly (A/cm^2), and i the PEMFC stack current density (A/cm^2).

The reversible voltage under different temperatures and pressures can be expressed as:

$$E_{rev} = N\left\{E^0 + \frac{RT}{2F}\ln\left[\frac{P_{H_2}(P_{O_2})^{\frac{1}{2}}}{P_{H_2O}}\right] + \frac{\Delta\overline{s}_{298.15K}}{nF}(T-298.15)\right\} \qquad (2)$$

where P_i is the partial pressure of species i (i is H_2, O_2/air, or liquid water at cathode side) (kPa), E^0 the cell open-circuit voltage (OCV) at the Standard Temperature and Pressure (STP), $E^0 = 1.23V$, and $\Delta\overline{s}_{298.15K}$ the change in the molar entropy at STP

(J/mol·K).

According to the above voltage output equation and electrochemical reaction principle, an equivalent circuit model and electrochemical generation steps of electricity in PEMFC are obtained, as shown in Fig. 2, where R_{fa} and R_{fc} are the anode and cathode Faradaic resistances ($\Omega \cdot cm^2$), reflecting the kinetics of the electrochemical reaction; C_{dla} and C_{dlc} are the anode and cathode double-layer capacitances (F), reflecting the capacitance feature of the electrochemical reaction interface, respectively. Z_W is the porous bounded Warburg impedance, modeling the mass transport in PEMFC, and it can be expressed as [22]:

$$Z_W = \frac{\sigma_i}{\sqrt{\omega}}(1-j)\tanh\left(\delta\sqrt{\frac{j\omega}{D_i}}\right) \tag{3}$$

where j is the imaginary part in a complex frequency domain coordinate system, δ the diffusion layer thickness (m), D_i the diffusion coefficient of species i (m^2/s), and σ_i the Warbury coefficient for species i (H$_2$, O$_2$/air, N$_2$, and H$_2$O), characterizing the effectiveness of transporting species i to or away from a reaction interface. The Warbury coefficient is defined as:

$$\sigma_i = \frac{RT}{\sqrt{2}A(n_iF)^2}\left(\frac{1}{c_i^0\sqrt{D_i}}\right) \tag{4}$$

where A is the cathode electrode area (m^2), c_i^0 the cathode bulk concentration of species i (mol/m^3), and n_i the number of electrons per molecule of species i.
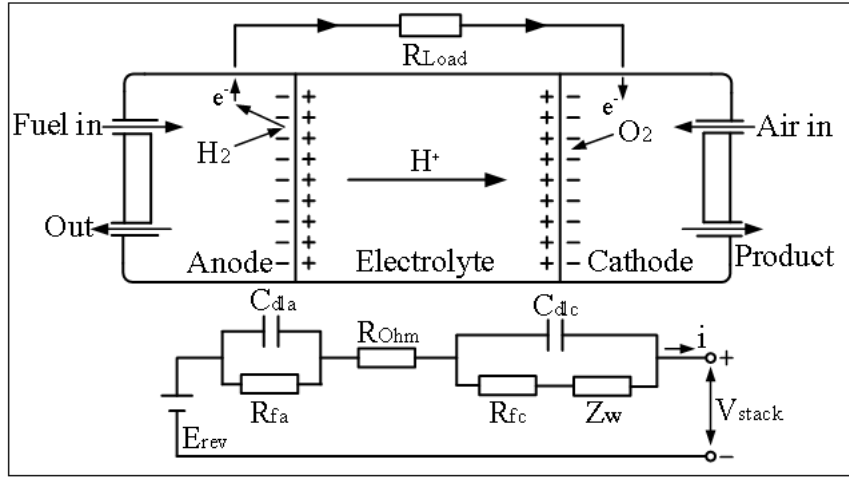
1

2   Fig. 2.   Equivalent circuit diagram and electrochemical generation steps of electricity in a PEMFC.

3   **3. LFCR production mechanism**

4   According to the electrochemical impedance spectroscopy analysis methods and

5   equivalent circuit model of PEMFC stack, it is assumed that the PEMFC must meet the

6   requirement of a linear system, and it is guaranteed by the amplitude of disturbance

7   signals injected into the PEMFC. Then, the fluctuation signal can be conducted in either

8   the galvanic-static mode or the potential-static mode [23].

9   As mentioned above, when the LFCR is injected into a PEMFC stack and produces

10   harmful influences on the FC current and voltage, the output current of the PEMFC

11   stack can be expressed as:

12

13     $i = I_{DC} + I_{BUS}\sin(2\omega t + \theta)$ (5)

14

15   where I_{DC} indicates the DC side current value of the DC/DC converter load, I_{BUS}, ω,

16   and θ are the amplitude, angular frequency and phase of the perturbation signal

1   (including the LFCR) from DC/DC converter, respectively.

2   According to the equivalent circuit model without LFCR injected into the PEMFC,

3   as shown in Fig. 2, the total AC impedance can be obtained as:

4

5    $$Z(j\omega) = R_{Ohm} + \frac{R_{fa} \cdot \dfrac{1}{j\omega C_{dla}}}{R_{fa} + \dfrac{1}{j\omega C_{dla}}} + \frac{(R_{fc} + Z_W) \cdot \dfrac{1}{j\omega C_{dlc}}}{R_{fc} + Z_W + \dfrac{1}{j\omega C_{dlc}}} \qquad (6)$$

6

7   When a PEMFC is injected by LFCR, $Z_W\big|_{\omega \to 0} = R_{conc} = \delta\sigma_i\sqrt{\dfrac{2}{D_i}}$, where R_{conc} is

8   known as the concentration resistance reflecting the mass transfer in PEMFC, Equation

9   (6) becomes:

10
$$Z'(j\omega) = R_{Ohm} + \frac{R_{fa} \cdot \dfrac{1}{j\omega C_{dla}}}{R_{fa} + \dfrac{1}{j\omega C_{dla}}} + \frac{(R_{fc} + R_{conc}) \cdot \dfrac{1}{j\omega C_{dlc}}}{R_{fc} + R_{conc} + \dfrac{1}{j\omega C_{dlc}}}$$

$$= R_{Ohm} + \frac{R_{fa}}{1+\omega^2\tau_a^2} + \frac{R_{fc} + R_{conc}}{1+\omega^2\tau_c^2} - j\left[\frac{\omega\tau_a \cdot R_{fa}}{1+\omega^2\tau_a^2} + \frac{\omega\tau_c(R_{fc} + R_{conc})}{1+\omega^2\tau_c^2}\right] \qquad (7)$$

$$= A(\omega)\angle\phi(\omega)$$

11   where $\tau_a = C_{dla}R_{fa}$ is the anode time constant (s), $\tau_c = C_{dlc}(R_{fc} + R_{conv})$ is the cathode

12   time constant (s), and $A(\omega)$ and $\phi(\omega)$ are the amplitude and phase shift resulted

13   from $Z(j\omega)$, respectively.

14   Fig. 3 shows the measured AC impedance variation of a 300 W self-humidified,

15   air-breathing, 63-cell PEMFC from Horizon Fuel Cell Technologies in Singapore, with

16   frequency from 0 to 200 Hz under the rated power conditions. Moreover, the lower the

17   frequency of current ripples, the higher the impedance of the PEMFC. Therefore, the

1 LFCR and harmonics will cause detrimental effects on the PEMFC performance.

2 The AC impedance tests of the 300 W PEMFC were performed using a

3 programmable high power DC electronic load (IT8902A/E-150-200), a function

4 generator, and a computer data-acquisition system equipped with corresponding

5 software, as shown in Fig. 4 . The AC impedance measurement method is that the rated

6 power condition is set in constant current (CC) mode as the DC current test point of the

7 PEMFC. The sinusoidal signal of test frequency is output by signal generator, the sine

8 waveform of electronic load is controlled, the voltage and current data in the internal

9 cache area of electronic load is read, and the fast Fourier transform (FFT) analysis is

10 carried out. Finally, a mathematical function is used to divide the converted voltage by

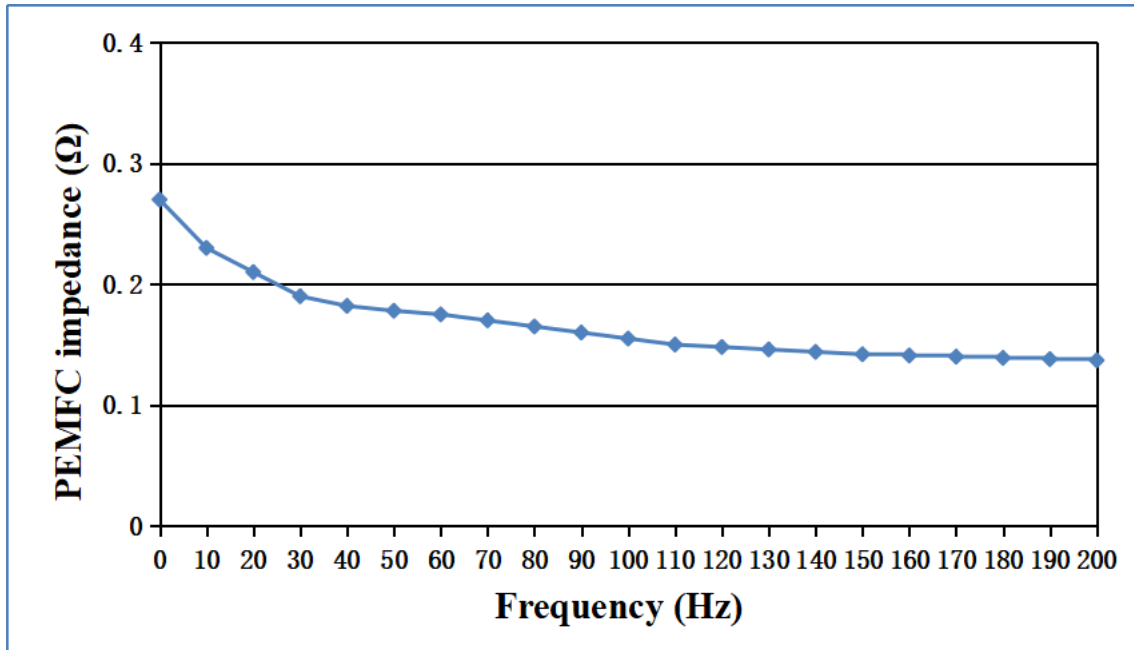11 the converted current to obtain the AC impedance of the PEMFC.

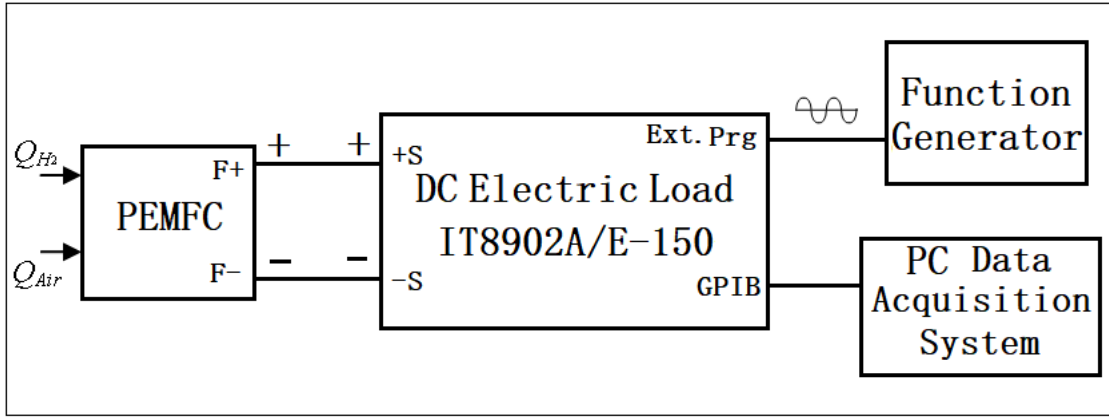13 Fig. 3. Impedance variation of a 300 W PEMFC at the rated conditions.

Fig. 4.　Schematic digram of PEMFC AC impedance measurement.

When the LFCR and harmonics are added to the PEMFC, the output voltage V_{stack} can be defined as:

$$V_{stack} = E_{rev} - N(R_{Ohm} + R_{fa} + R_{fc} + R_{conc})I_{DC} \\ - NA(\omega)I_{BUS}\sin(\omega t + \theta + \phi)$$

(8)

Consequently, it could be analyzed that the LFCR is reflected into PEMFC stack and brings harmful influences on the FC stack.

4. Experimental results and discussion

The experimental setup consists of a UPS system, PEMFC power generation and test system, lead-acid batteries, supercapacitors, and a data-acquisition system. In the PEMFC power generation and test system, a hydrogen flowmeter F-201C-GAS-22V (Bronkhorst) and an air flowmeter F-112AC-GAS-22V (Bronkhorst) are selected. The temperature and humidity of hydrogen and air are controlled by the hydrotransmitter HD2008TV1 (Delta OHM), and the pressure transmitter between the inlets of cathode

1 and anode is the AUS EX 1354X (Burkert). All the physical parameters, such as the

2 performance, lifetime, power and efficiency, heat and temperature, fuel consumption

3 and utilization are recorded with the data-acquisition system. Voltage and current

4 signals are measured by using an LA55-P and an LV25-P [24].

5   Fig. 5 shows a photo of the new experimental setup at the University of
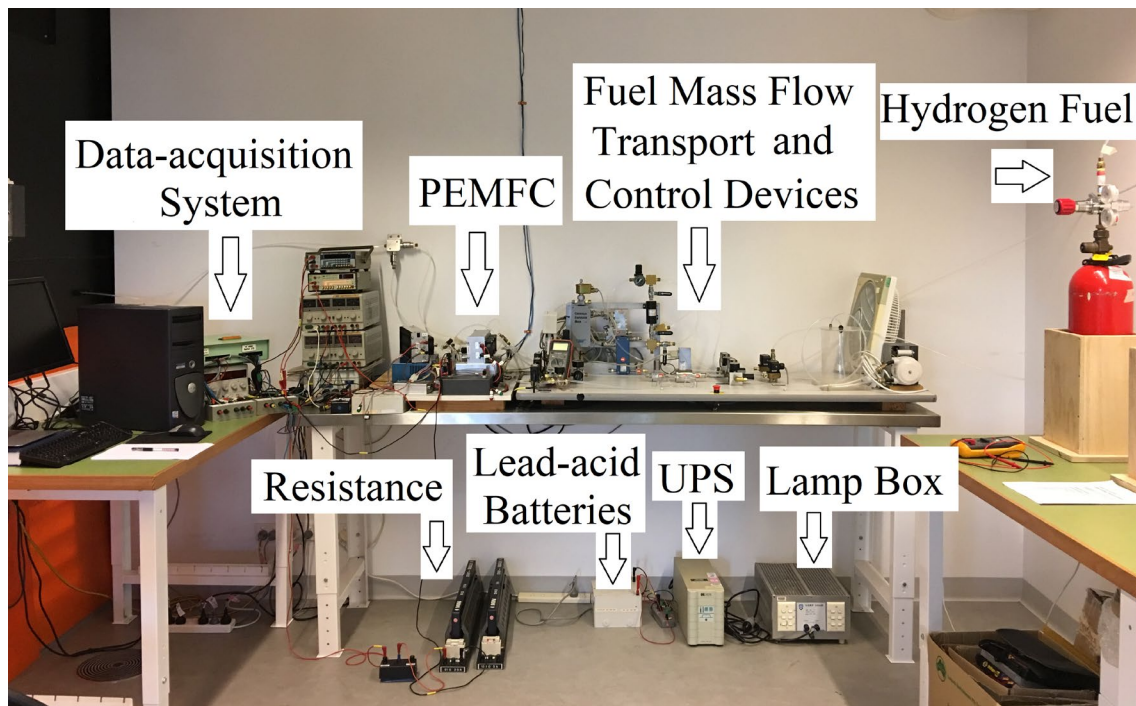
6 Technology Sydney (UTS), Australia.

7

8 Fig. 5.   Photograph of the new experimental setup.

9

10 4.1. Influence of LFCR on PEMFC stack **performance**

11   The LFCR injected into a PEMFC will influence the voltage-current performance,

12 which can be calculated from the mathematical model mentioned above and tested via

13 the experiments, as shown in Fig. 6, where one is with LFCR, and the other is without

14 LFCR. Fig. 6 illustrates the performance degradation of PEMFC with LFCR, compared

15 to that without LFCR. When there are perturbation signals, including the LFCR and

harmonics from the PCS, compared with the case of no perturbation signal, the

performance of PEMFC stack can be changed because of the AC component in

Equation (7). Furthermore, the enclosed area represents the performance degradation of

PEMFC because of the influence of LFCR and harmonics. That is the additional system
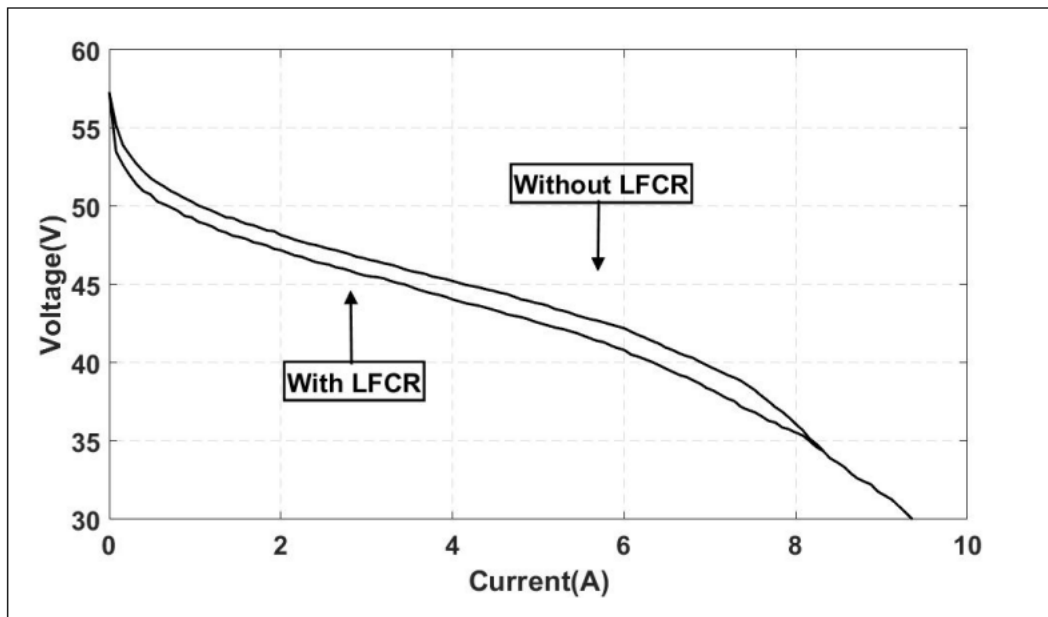
loss because of the action of $Z(j\omega)$ [5].

Fig. 6.   Voltage-current curve of a 300 W PEMFC stack obtained for the ascending and descending
branches for the inversion point I= 8.2 A.

4.2. Influence on FC stack lifetime

The PEMFC is a complex electrochemical device, which constitutes many

components, such as catalysts, catalyst supports, proton exchange membranes, gas

diffusion layers (GDLs), bipolar plates, sealings and gaskets. Each of these components

could degrade or fail, leading to the FC system to degrade or fail.

In a designed PEMFC PCS, the LFCR and harmonics will decrease the FC lifetime.

Fig. 7 depicts the measured results of stack voltage versus time for two different cases

with and without LFCR when a 300 W PEMFC PGS is connected to a resistive load or a

UPS load with a DC/DC converter. As shown in Fig. 7, the lifetime of PEMFC with LFCR is shorter than that without LFCR.
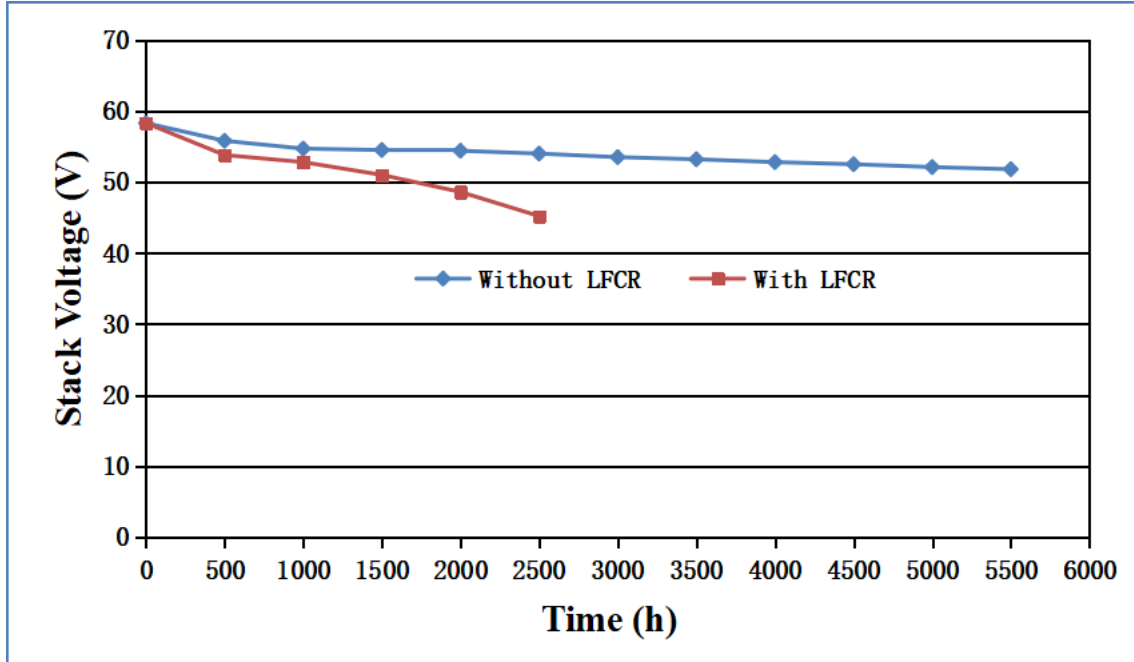

Fig. 7.   Different lifetimes and performances of PEMFC stack with and without LFCR.

As mentioned above, the LFCR can produce influences of the performance degradation and lifetime on PEMFC, because it has a great influence on the anode and cathode double layer capacitor in the electrochemical reaction interface of PEMFC and causes many other issues. The degradation of PEMFC basically involves the mechanical degradation, chemical or electrochemical degradation, thermal degradation, and material degradation through the action of the perturbation signal, such as LFCR and harmonics, resulting in the static and dynamic performance degradation of PEMFC. Moreover, it can increase the power loss and heat, and even reduce the FC durability and reliability. The conclusion could be obtained according to the equivalent circuit model of a PEMFC considering the degradation influences.

On the other hand, the component degradation includes that, but is not limited to, (1) in catalyst, there are the platinum catalyst degradation of Pt agglomeration and particle growth, Pt migration, Pt elemental loss, Pt catalyst contamination, and catalyst support degradation, (2) in membrane, there are the membrane degradation on chemical aspect and mechanical aspect, pinholes, delamination, and cracking of membrane, (3) in porous transport layer, there are the degradation on mechanical and thermal physics aspect, chemical and electrochemical aspect, and porosity and pore size distributions, (4) in bipolar plates, there are the degradation of graphite composite bipolar plates and metal bipolar plates, and (5) in other components, there are the degradation of the seals, endplates, and bus plates [25].

Some degradation mechanisms for a PEMFC, such as the carbon corrosion for a typical Pt/C catalyst, the Pt particle growth and dissolution/precipitation, and the chain scission of perfluorosulfonic acid (PFSA) membrane, can offer deep understanding in the FC degradation. In addition, the degradation processes of different components are often related to the materials, control and design of an FC system. Therefore, it is important to investigate, analyze, and systematically understand the degradation phenomena of each component, so that some novel component materials and manufacture technologies can be developed. Furthermore, the novel modeling, control and design from cells to stacks can be achieved to mitigate the negative influences on the FC durability and reliability under all kinds of operation conditions.

According to the 2016 US Department of Energy (DOE) report, the lifetime and cost

targets are to develop a 65% peak-efficient, direct hydrogen FC power system for transportation that can achieve 5,000 h durability (ultimate 8,000 h) and be mass produced at a cost of $40/kW by 2020 (ultimate $30/kW) [26]. Therefore, further investigation for improving the PEMFC performance and prolonging the lifetime of PEMFC seems to be necessary.

4.3. Influences on FC stack efficiency and power

Based on the electrochemical principle, assuming that all of the Gibbs free energy can be converted into electrical energy, in theory, the maximum possible electrochemical efficiency of an FC is the ratio between the Gibbs free energy and hydrogen higher heating value, or $\eta_{Theory} = \Delta G / \Delta H = 237.34 / 286.02 = 83\%$.

In practical application, because of various possibilities, such as the hydrogen diffusion through the membrane, combining with oxygen diffused through the membrane, and internal currents, some hydrogen is lost. On the other hand, due to the hydrogen stoichiometry ratio in the electrochemical reaction, the hydrogen consumption will be higher than that corresponding to the current generated, and the FC efficiency would be lower than given theoretical value. The FC efficiency is then [22]:

$$\eta_{FC} = \frac{V_{Stack}}{1.482} \left(\frac{i}{i + i_{loss}} \right) \eta_{fu} \tag{9}$$

where η_{fu} is the fuel utilization, and i_{loss} the hydrogen loss current (A/cm^2).

Consequently, when a pure resistive load is connected to the 300W PEMFC generation system without using PCS in the experiment, its measured efficiency η_{FC} is about 45%~55%, as shown in Fig. 8.
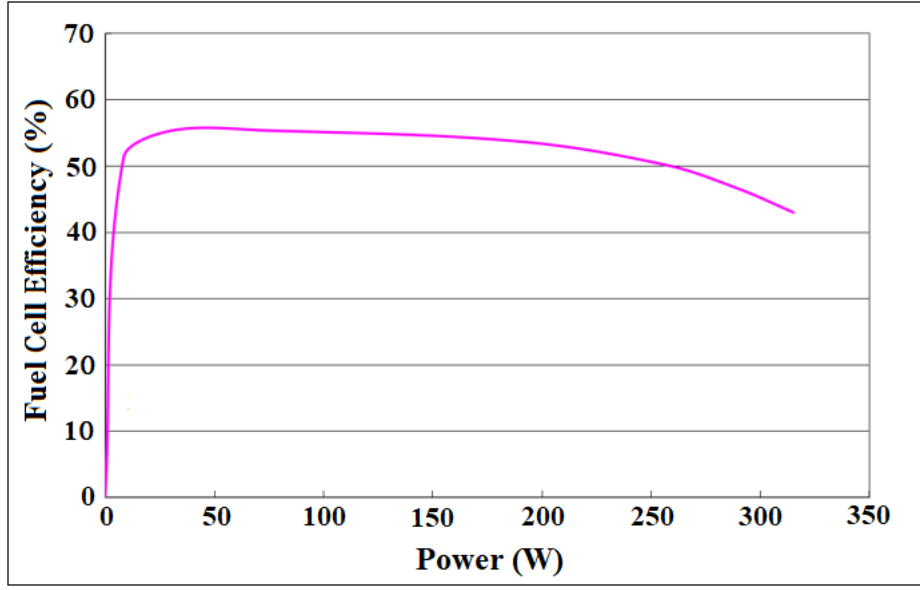
Fig. 8.　Efficiency of a 300 W PEMFC stack without PCS.

When the PCS is used in the PEMFC power system, the overall efficiency of FC PCS system is

$$\eta_{sys} = \eta_{FC}\eta_{PCS}\eta_{ripple} \tag{10}$$

where η_{ripple} is the ripple efficiency of an FC associated with current ripples and harmonics, and η_{PCS} the efficiency of DC/DC or DC/AC power converter in PCS. According to the measured value of the FC PCS system, the efficiency of PCS in PEMFC operating mode under the rated load of 270 W is $\eta_{PCS} = \eta_{DC/DC}\eta_{DC/AC} = 72\%$.

The definition of an FC efficiency associated with current ripple is:

$$\eta_{ripple} = \frac{P_{Out}}{P_{Bus}} = 1 - \frac{P_{Ripple}}{P_{Bus}} \tag{11}$$

where $P_{Out} = P_{Bus} - P_{Ripple}$, $P_{Bus} = V_{Bus}I_{Bus}$ is the output power in the DC bus side and $P_{Ripple} = |Z(j\omega)|I_{Ripple}^2$ represents the additional losses due to the current ripple itself.

Therefore, when the PEMFC is connected to the DC/DC converter without any mitigation control methods of LFCR and harmonics, the $|Z(j\omega)|$ will increase, and the

17

1 ripple current value will produce a ripple power loss. The practical output power of

2 PEMFC will decrease. Fig. 9 illustrates the PEMFC stack efficiency measured as a

3 function of ripple frequency of 50 Hz to 400 Hz and ripple amplitudes of 9.9% (when

4 using a passive compensation method in PEMFC PCS), and 24.3% (without any

5 compensation methods in PEMFC PCS) in the rated load (about 8.20 A). As expected in

6 Fig. 9, the curves show that the efficiency of PEMFC stack decreases as the ripple

7 amplitude increases, and an increase in the ripple frequency helps to increase the

8 efficiency, and reduce hydrogen fuel utilization. On the contrary, the high frequency

9 ripple currents, such as DC/DC converter switching at a frequency of 50 kHz, can be

10 greatly weakened by the input capacitor, which has little or no influence on PEMFC
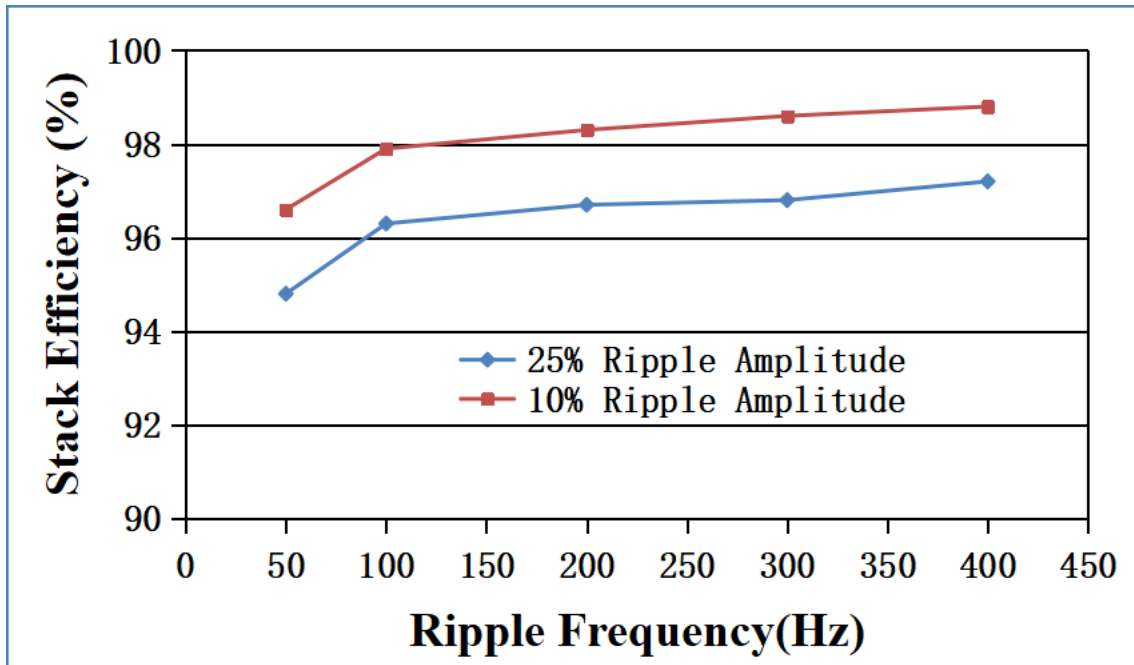
11 efficiency.

12

13　Fig. 9.　Influences of different percentage amplitudes of LFCR on PEMFC stack efficiency.

14　　Figs. 10(a) and 10(b) show the measured input power and current curves of the

15 PEMFC with a pure resistive load and a DC/DC converter load, respectively, in a UPS

1   system under the same operation conditions. The output power of PEMFC with LFCR

2   and harmonics with the DC/DC converter load is about 1.3%～2.6% more than that of

3   PEMFC with a pure resistive load. Moreover, when the UPS without any load is

4   connected to a running PEMFC, a 35 W power has been lost, as shown in Fig. 10(b). In

5   Fig. 10(b), with the increase of the UPS load that has the same power as the resistance

6   load, its power loss range of PEMFC stack is from 37 W to 49 W, which includes the

7   power loss caused by the current ripple. Furthermore, the maximum output powers of

8   PEMFC are 338 W and 371 W when connected to UPS system and resistance load,

9   respectively. Therefore, the load ability of PEMFC connected to UPS system is poorer.

10
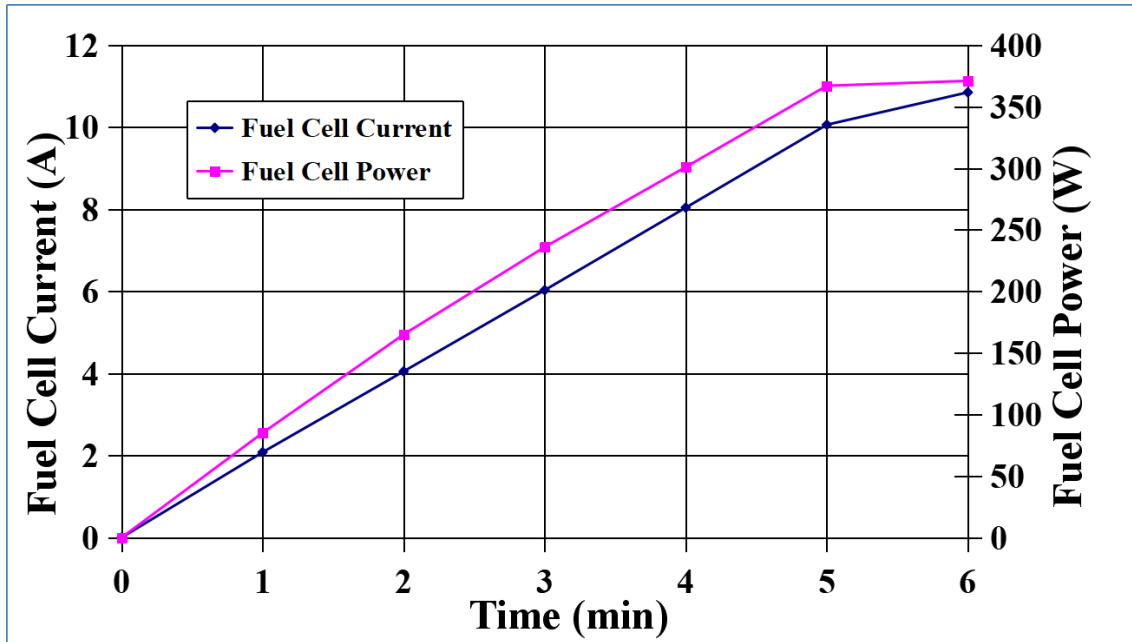
11   (a)
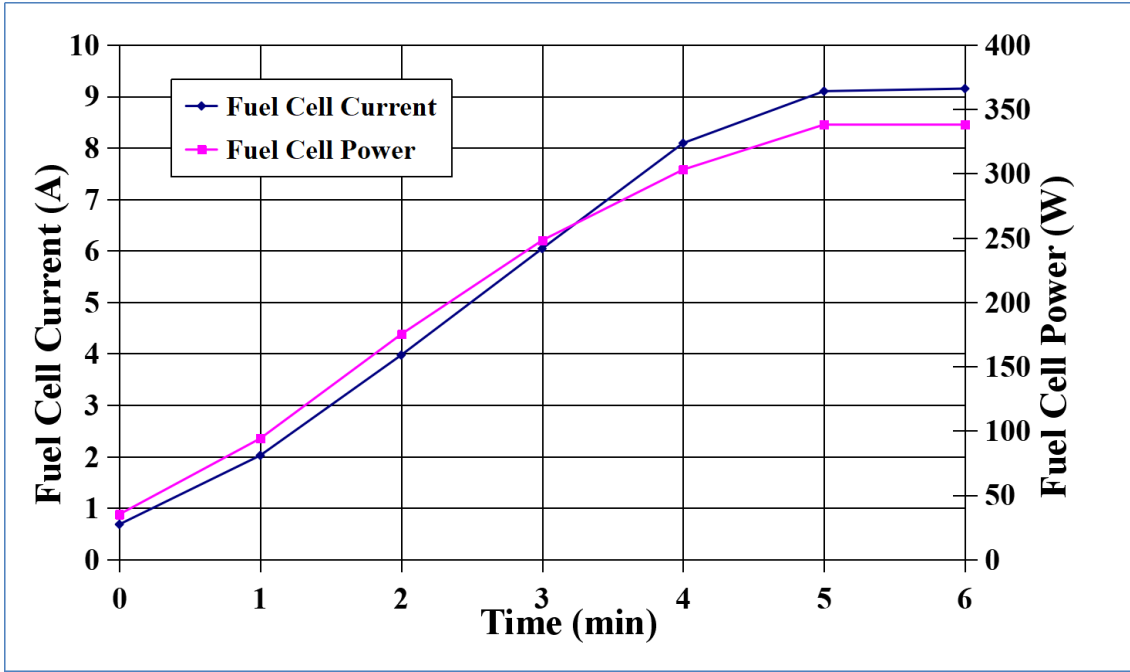
(b)

Fig. 10.　Power and current characteristics of PEMFC under different types of loads: (a) pure resistive load, and (b) UPS system with DC/DC converter.

4.4. Influences of LFCR on fuel utilization

According to the definition, the fuel utilization η_{fu} in an FC power system can be expressed as:

$$\eta_{fu} = \frac{\dot{n}_{cons}}{\dot{n}_{cons} + \dot{n}_{loss} + \tau_{prg} f_{prg} \dot{n}_{purge}} \qquad (12)$$

where $\dot{n}_{cons}$ is the mass flow rate of fuel consumption (mol/s), $\dot{n}_{loss}$ the mass flow rate of fuel loss (mol/s), $\dot{n}_{purge}$ the mass flow rate of fuel purge (mol/s), τ_{prg} the duration of fuel purge (s), and f_{prg} the frequency of fuel purge (Hz).

In general, the fuel utilization is related to the fuel stoichiometric ratio. For instance, the hydrogen utilization η_{H_2} can be obtained from the current drawn by FC

1   power system as shown in the following expression:

2     $$\eta_{H_2} = \frac{1}{S_{H_2}}$$ (13)

3   where S_{H_2} is the hydrogen stoichiometric ratio, and $S_{H_2} = \dfrac{\dot{n}_{H_2.act}}{\dot{n}_{H_2.theory}} = \dfrac{nF}{I}\dot{n}_{H_2.act}$.

4   Therefore, the hydrogen utilization, η_{H_2}, oxygen utilization, η_{O_2}, and air

5   utilization, η_{Air}, can be obtained from the current drawn by FC power system by using

6   the following expression:

7     $$\eta_{H_2} = \frac{I}{nF\dot{n}_{H_2}}$$ (14)

8   where I is the FC output current (A), $\dot{n}_{H_2}$ the hydrogen mass flow rate (mol/s), and

9   nF determines the charge flow between the anode and the cathode. In the same manner,

10   the oxygen and air utilization can be obtained as follows:

11    $$\eta_{O_2} = \frac{I}{nF\dot{n}_{O_2}}$$ (15)

12    $$\eta_{Air} = \frac{I}{nF\dot{n}_{Air}}$$ (16)

13   For the pure hydrogen and the dead-end purge mode, because S_{H_2}=1.1 to 1.2,

14   S_{O_2}=1.2 to 1.5, and S_{Air}=2 to 2.5, one can obtain that η_{H_2}=83.3% to 90.9%, η_{O_2}=

15   66.7% to 83.3%, and η_{Air}=40% to 50%. However, to improve the performance of FC,

16   the fixed cycle of purge mode has to be used in FC power system. At this point, it is

17   difficult to measure the fuel utilization accurately.

18   The influence of fuel utilization on the FC output voltage is because of the LFCR

19   and harmonics injected. Fig. 11 shows the impact of fuel utilization on the 300 W

PEMFC output voltages due to the LFCR and harmonics. The larger the initial fuel utilization, the larger the reactant consumption.
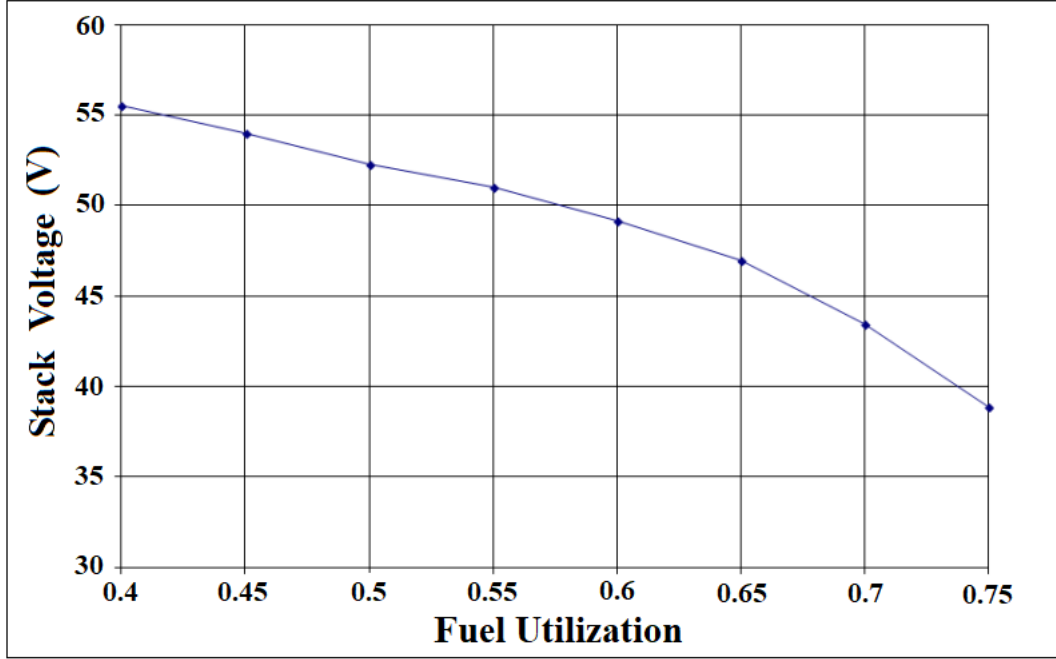

Fig. 11.   Impact of initial hydrogen utilization on fractional voltage drop.

4.5. Influence of LFCR on FC stack heat and temperature

In an FC, the internal heat transfer is derived from the electron transmission and ion transport behavior of electrochemical reaction resistance. Assure that the water within the FC is vaporized, and the steam produced has been removed out of FC, the heat flow q_{int} is generated by:

$$q_{\text{int}} = R_{Ohm} i^2 \tag{17}$$

When the LFCR is injected into the FC, it makes the resistance of PEMFC change, $R_{Ohm} \to R_{ripple}$, as shown in Fig. 3, the heat produced will increase as follows:

$$\Delta q_{\text{int}.ripple} = R_{ripple} i^2 \tag{18}$$

1   To keep the water balance and reduce the influence of the internal resistance or

2   Ohmic losses, the stack temperature will be controlled in the range of 50~60°C under

3   the rated load, as shown in Figs. 12(a) -12(c). In this experiment, when the load changes

4   as mentioned in Fig. 12(a), the stack temperature and fan velocity show that the

5   characteristics of temperature and fan velocity when connected to a resistive load are

6   smoother than those when connected to a UPS system with a DC/DC converter or

7   DC/AC inverter. However, in the steady state, the former's temperature and fan velocity,

8   as shown in Fig. 12(b), are smaller than those of the latter, as depicted in Fig. 12(c).

9
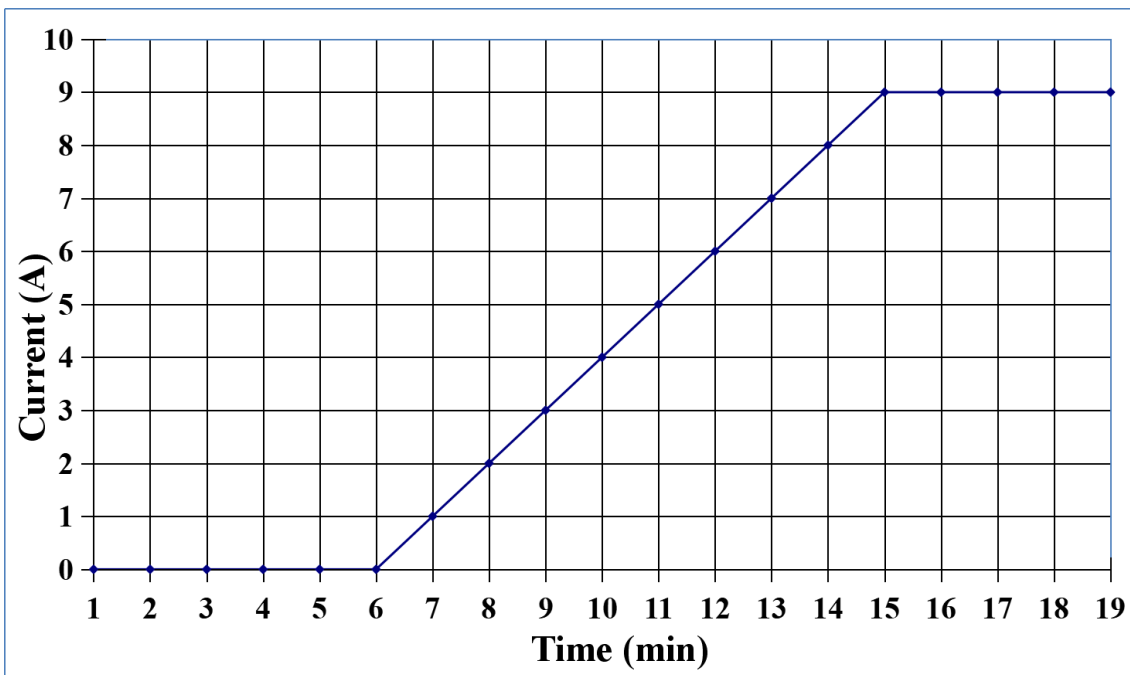
10   (a)
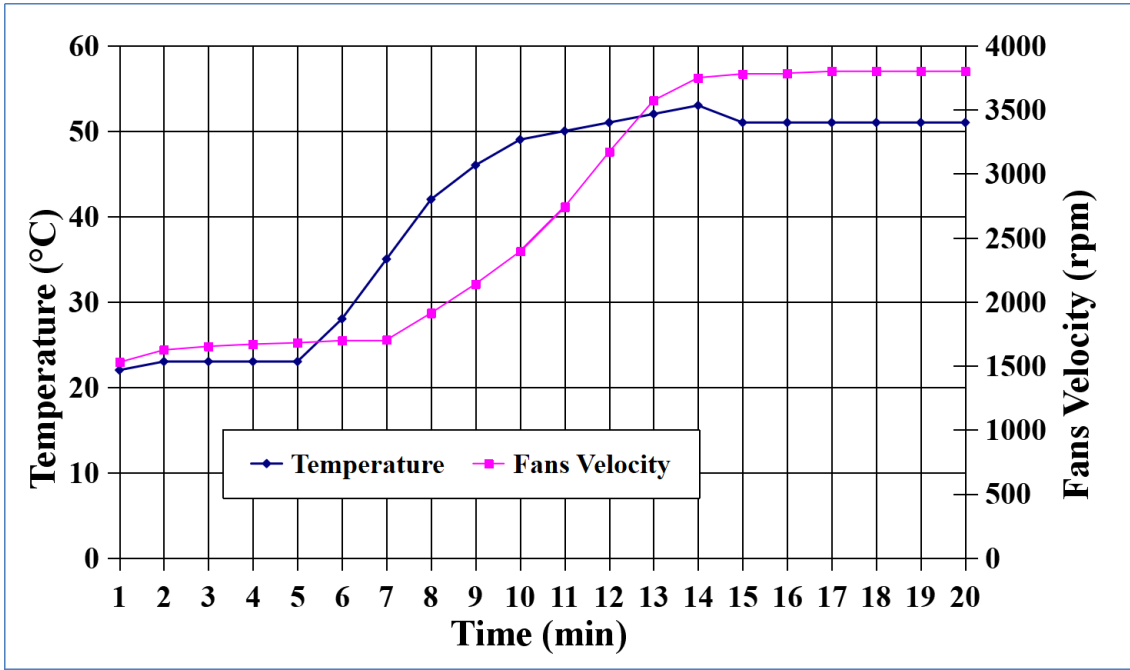
(b)
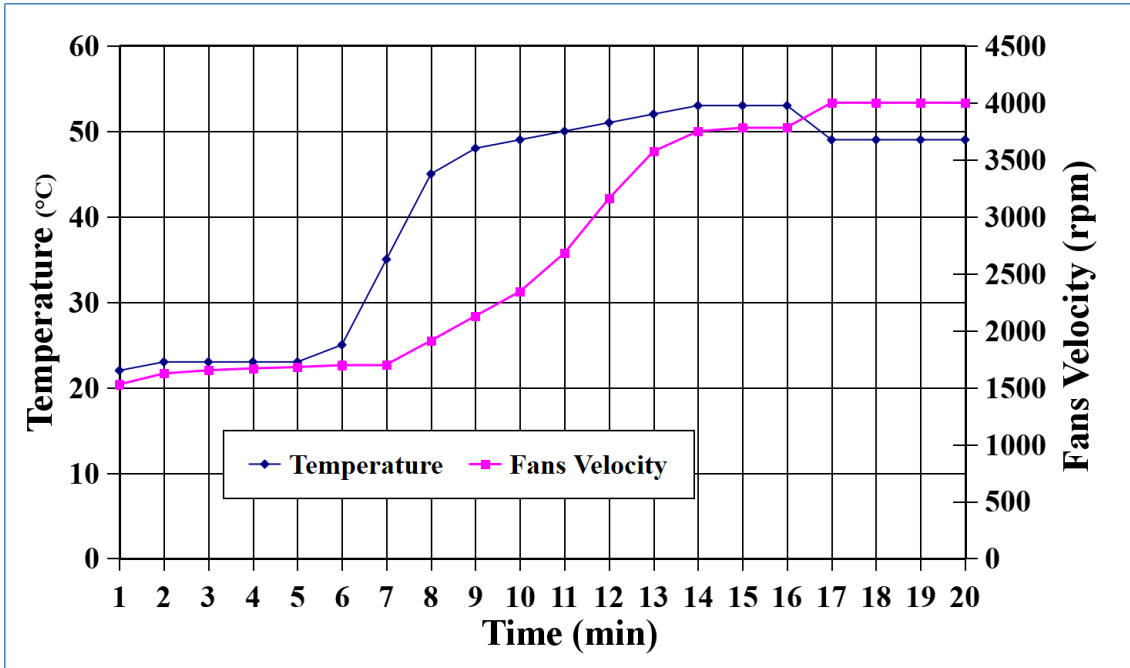
(c)

Fig. 12.   PEMFC stack temperature and fan velocity charts under: (a) load variations, (b) resistance

load, and (c) UPS load.

According to Equation (18), the heat produced in the PEMFC, if not managed and

dissipated properly, can have a significant influence on the performance and lifespan of the FC. The variations occur in the hydrogen utilization and the temperature of an air supply pipe (ASP) with the ripple amplitude and frequency of the current in SOFC PCS. The hydrogen utilization has to increase significantly to meet higher load demands. Moreover, The ASP temperature varies with the load. Therefore, the influence of such load transients on SOFC temperature distribution could be illustrated [13].

5. Conclusion

In this paper, using an equivalent circuit modeling and comprehensive analysis methodology, the influences of LFCR on a PEMFC performance, lifetime, power and efficiency, heat and temperature, fuel consumption and utilization are analyzed and discussed. A 300 W PEMFC UPS prototype is implemented with an input voltage range from 30 to 60 V. The experimental results show that the LFCR with large magnitudes related to the angular frequency and phase of the perturbation signal from DC/DC converter and DC/AC inverter in the UPS system result in the decreased variations in the performance, lifespan, power and efficiency of a PEMFC, and increased variations in the thermal and temperature, fuel consumption and utilization of the PEMFC.

REFERENCES

[1] Gautam AR, Gourav K, Guerrero JM, Fulwani DM. Ripple mitigation with improved line-load transients response in a two-stage DC–DC–AC converter: adaptive SMC approach. IEEE T Ind Electron 2018; 65(4): 3125-35.

[2] Sha DS, Xu YX, Zhang JK, Yan Y. Current-fed hybrid dual active bridge DC-DC converter for a fuel cell power conditioning system with reduced input current ripple. IEEE T Ind Electron 2017; 64(8): 6628-38.

[3] Gemmen RS. Analysis for the effect of inverter ripple current on fuel cell operating condition. J Fluids Eng 2003; 125(3): 576-85.

[4] NETL. Fuel Cell Specifications for Future Energy Challenge 2010 Competition. http://www.netl.doe.gov (accessed 2.07.2010).

[5] Ksiazek PF, Ordonez M. Swinging bus technique for ripple current elimination in fuel cell power conversion. IEEE T Power Electron 2014; 29 (1): 170-78.

[6] Ferrero R, Marracci M, Tellini B. Single PEM fuel fell analysis for the evaluation of current ripple effects. IEEE T Instrumentation and Measurement 2013; 62(3): 1058-64.

[7] Choi WJ, Howze WJ, Enjeti P. Development of an equivalent circuit model of a fuel cell to evaluate the effects of inverter ripple current. J Power Sources 2006; 158(2): 1324-32.

[8] Ferrero R, Marracci M, Priol M, Tellini B. Simplified model for evaluating ripple effects on commercial PEM fuel cell. Int J Hydrogen Energy 2012; 37(18): 13462-69.

[9] Wahdame B, et al. Impact of power converter current ripple on the durability of a fuel cell stack. ISIE 2008 Conference, Cambridge, England, 30 Jun-2 Jul 2008; 1495-500.

[10] Sergi F, et al. PEM fuel cells analysis for grid connected applications. Int J Hydrogen Energy 2011; 36(17):10908-16.

[11] Kim JS, Choe GY, Kang HS, Lee BK. Robust low frequency current ripple elimination algorithm for grid-connected fuel cell systems with power balancing technique. Renewable Energy 2011; 36(5): 1392-400.

[12] Mazumder SK, Burra RK, Acharya KA. Ripple-mitigating and energy-efficient fuel cell power-conditioning system. IEEE T Power Electron 2007; 22(4): 1437-52.

[13] Mazumder SK, et al. Solid-oxide-fuel-cell performance and durability: resolution of the effects of power-conditioning systems and application loads. IEEE T Power Electron 2004; 19(5): 1263-78.

[14] Wai RJ, Chun YL. Dual active low-frequency ripple control for clean-energy power-conditioning mechanism. IEEE T Ind Electron 2011; 58(11): 5172-85.

[15] Mayo-Maldonado JC, et al. A novel PEMFC power conditioning system based on the interleaved high gain boost converter, Int J Hydrogen Energy 2019; 44(24): 12508-14.

[16] Wang HQ, Gaillard A, Hissel D. Online electrochemical impedance spectroscopy detection integrated with step-up converter for fuel cell electric vehicle, Int J Hydrogen Energy 2019; 44(2): 1110-21.

[17] Bankupalli PT, Ghosh S, Kumar L, Samanta S. Fractional order modeling and two loop control of PEM fuel cell for voltage regulation considering both source and load perturbations, Int J Hydrogen Energy 2018; 43(12): 6294-307.

[18] Ramirez-Murillo H, Restrepo C, Konjedic T, Calvente J, Romero A, Baier C, Gira R. An efficiency comparison of fuel-cell hybrid systems based on the versatile buck-boost converter, IEEE T Power Electron 2018; 33(2): 1237-46.

[19] Shireen W, Nene HR. Input ripple current compensation using DSP control in reliable fuel cell power systems, Int J Hydrogen Energy 2012; 37(9): 7807-13.

[20] Somaiah B, Agarwal V, Choudhury SR, Duttagupta SP, Govindan K. Analysis and comparative study of pulsating current of fuel cells by inverter load with different power converter topologies, Int J Hydrogen Energy 2011; 36(22): 15018-28.

[21] Hong P, Li JQ, Xu LF, Yang MG, Fang C. Modeling and simulation of parallel DC/DC converters for online AC impedance estimation of PEM fuel cell stack. Int J Hydrogen Energy 2016; 41(4): 3004-14.

[22] Barbir F. FEM Fuel Cell: Theory and Practice, New York: Elsevier Academic Press, 2005.

1 [23] Kim JS, Choe GY, Kang HS, Lee BK. Effect of load modeling on low frequency

2   current ripple in fuel cell generation systems. J Electrical Engineering &

3   Technology 2010; 5(2): 307-18.

4 [24] Zhan YD, Guo YG, Zhu JG, Wang H. Intelligent uninterruptible power supply

5   system with backup fuel cell/battery hybrid power sources. J Power Sources 2008;

6   179(2): 745-753.

7 [25] Wang HJ, Li H, Yuan X. PEM Fuel Cell Failure Mode Analysis, New York: CRC

8   Press, 2012.

9 [26] 2016 Annual Progress Report of US Department of Energy (DOE): V.0 Fuel Cells

10   Program Overview, June 2016.

11 https://www.hydrogen.energy.gov/pdfs/progress16/v_0_papageorgopoulos_2016.pdf

12

13

14

15